

Development of a System to Measure Radius of Curvature and Speed of Hammer Head during Turns in Hammer Throw

Koji MUROFUSHI*, Shinji Sakurai**, Koji Umegaki*** and Kazutoshi Kobayashi**

*Chukyo University Graduate School of Health and Sport Sciences
101 Tokodachi, Kaizu-cho, Toyota, Aichi 470-0393 Japan
kojimuro@cnc.chukyo-u.ac.jp

**Chukyo University Department of Sport Science
101 Tokodachi, Kaizu-cho, Toyota, Aichi 470-0393 Japan

***Maizuru National Collage of Technology Natural Science Studies
234 Shiroya, Maizuru, Kyoto 625-8511 Japan

[Received September 3, 2004 ; Accepted February 28, 2005]

The aim of this study was to compare the radius of curvature and the estimated head speed as measured by sensors attached to a hammer with those calculated by video image analysis. The participant was the Japanese record holder(83m47). He threw a hammer with sensors which measured the force exerted along the length of the hammer cable using a tension meter made of a metal plate to which strain gauges were affixed, and the angular velocity perpendicular to the hammer cable using two IC accelerometers whose axes were aligned together with the hammer cable. The radius and speed obtained using the sensors were similar to those obtained from video analysis in values, but were slightly out of phase. This is because measuring the angular velocity by sensors eliminates translational motion and only produces results for rotational motion. The length of time required to obtain these results was shortened by the use of a hammer with sensors. Therefore, the system using sensors attached to a hammer will enable athletes and coaches to interpret the data about each throw while it is still fresh in their minds.

Keywords: accelerometer, tension meter, sensor, angular velocity

[International Journal of Sport and Health Science Vol.3, 116-128, 2005]

1. Introduction

The hammer throw is an event in which a competitor tries to throw the hammer, a 16-pound (7.26 kg) ball attached to a handle with a length of piano wire (a length of 117.5 to 121.5 cm from ball to the inside of the handle), as far as possible within an arc of 35° from a concrete circle with a diameter of 2.13 m, combining a rotational movement with a translational movement. It is possible to say that the throwing distance is determined at the instant of release. The factors involved in determining the distance include the speed of the hammer head at the moment of release (speed of release), angle of release, height of release and air resistance, but of these the most important factor is speed of release (Murofushi, 1994).

For example, Murofushi (1982), standardizing the distance value at 80m80, with initial conditions of speed of release 28.2 m/s, angle of release 38° and height of release 1.7 m, ignoring air resistance, investigated the influence of speed of release, angle of release and height of release on distance through simulations. He reported results showing that changes in the speed of release had great influence, while the influence of changes in height of release was small. In addition, Ikegami et al. (1994) investigated the coefficient of correlation between the records and initial speed (speed of release), initial horizontal speed, initial vertical speed, angle of release, height of release and direction of release among the top six competitors at the Tokyo Athletics World Championship 1991. They report that the only significant correlation found was with initial speed,

and that even at such a world-class competitive level, initial speed is the point that determines victory or defeat.

Various factors have been suggested for increasing the speed of the hammer to raise the speed of release: for example, how much the body can be rotated ahead of the hammer, rotating faster through an increase in the radius of rotation by sufficiently stretching the arms and putting the shoulders forward (Ono 1957), moving the rotational axis, using gravity to pull with body weight (Dyson 1972), making the thrower-hammer system forward translational movement, lengthening and shortening the radius of rotation (Dapena 1984, 1985; Dapena and Feltner 1989). In addition, Payne (1990) reports on the extension of arc length and continuation of swinging by pumping of the knees when riding a swing or by the expansion and contraction of posture by adjusting the shoulder joints during the giant swing on the horizontal bar in gymnastics; he suggests that the same principle may be applicable to the hammer throw. Just as in the above-mentioned swing and gymnastics giant swing, it is necessary to study the changes in rotational radius by similar movements in the hammer throw (for example, postures in which the pull is from the hips by leaning the torso forward, or from the shoulders by leaning the torso back [Dapena and Feltner 1989]).

Generally speaking, the speed of rotational movement is determined by the product of the angular velocity of rotation and the radius of rotation. Also, the centripetal force (or the centrifugal force) is proportional to the square of the angular velocity of rotation and the radius of rotation, proportional to the square of the speed and inversely proportional to the radius of rotation. Lapp (1935) sought speed of release and angle of release from distance and flight time; positing an orbital radius of 5 feet for the hammer head (length of the hammer plus 1 foot, placing the center of rotation in the elbow area), he sought the centrifugal force from the average angular velocity of rotation and the speed of release. Since that research hammer throw studies focus not only on the speed of the hammer head and the centrifugal force, but also on the radius of rotation. In papers that investigated the rotational radius in the hammer throw, Kobayashi and Kaneko (1980), Yuasa et al. (1984) used 16 mm cine cameras from above and measured the radius of curvature by 2D image analysis. Umegaki and Mizutani (1997) conducted

3D analysis by DLT method and measured distance between the center of gravity of the thrower and the hammer head. Also, Dapena and Feltner (1989) determined the center point of rotation from the locus of the hammer head, leaving out the translational movement component of the thrower-hammer system, and sought an average value of radius for the turning radius for each turn. More recently, Gutierrez et al. (2002) conducted video image analysis on the competitors who advanced to the final round in the Seville Athletics World Championship 1999, seeking an average value for radius of curvature per turn and in single and double support phases. However, although image analysis permits the collection of data from real competition, it has problems in that it requires a great deal of time and patience for processing. If we could find out changes in radius of rotation during the hammer throw in real time or immediately after the throw, we might be able to return valuable information to coaches and competitors on the spot.

Therefore, in this study, we constructed a hammer equipped with sensors that can measure radius of curvature, with the aim of improving throwing techniques by offering data to coaches and competitors while practice is taking place. Next we compared the radius of curvature and the speed of the hammer head as measured by the sensor hammer with the same factors measured through the former video image method, and clarified the special characteristics of sensor measurement.

2. Methodology

2.1. Construction of the sensor to measure radius of curvature

2.1.1. Principle of the sensor

In the hammer throw, we believe that gravity acting on the hammer head is comparatively small compared to the cable force, so in this research we decided to ignore the effects of gravity on the hammer head. Centrifugal force F (N) in uniform rotational motion at any given moment of an object of mass m (kg) is:

$$F = m r \omega^2 \quad (1)$$

However, r (m): radius of curvature according to sensor; ω (rad/s): angular velocity according to sensor. From Formula 1, we determine radius of

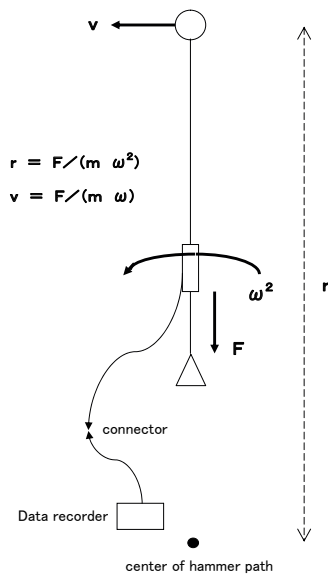


Figure 1 A diagram of the hammer which is equipped with a tension meter and accelerometers to measure a radius of curvature and to estimate a head speed at an instant.

curvature r according to sensor to be:

$$r = F / (m \omega^2) \quad (2)$$

Accordingly, as seen in **Figure 1**, we can measure the tensile force F working on the cable and the angular velocity ω ; if we already know the mass of the hammer m , it becomes possible to measure the radius of curvature r in the hammer throw via the sensor, and also the speed v (m/s). Since $v = r\omega$, if we substitute Formula (2) for r , the speed v of the hammer head is:

$$v = F / (m \omega) \quad (3)$$

Meanwhile, the radius of curvature as originally defined can be obtained as shown in the Appendix. In addition, the difference between the radius of curvature according to the sensor and the originally defined radius of curvature is also shown in the Appendix.

2.1.2. Tensile force sensor

In order to measure the radius of curvature r via sensor using the above principles, it is necessary to measure both the cable force F and the angular velocity ω simultaneously. In this research we employed an ordinary men's hammer to construct a sensor hammer capable of measuring tensile force and angular velocity at the same time. The weight of the hammer alone was 7.26 kg. In addition, the length from the handle to the head of the hammer was 120 cm. The tensile force sensor was placed on the wire between the handle and the head of the hammer. As can be seen in the upper portion of **Figure 2**, our homemade sensor was a stainless steel plate, 2.5 mm in thickness, 25 mm in width and 150 mm in length, with strain gauges attached to the center of both faces. The signals obtained from the sensor were passed through a strain preamplifier (AR-C2ST2: Teac Corp., weight 30 g) and recorded on a data recorder (DR-C2 PC Card Recorder: Teac Corp., thickness 28 mm, width 85 mm, length 135 mm, weight 320 g, total weight 440g including remote switch) (lower part of **Figure 2**).

2.1.3. Angular velocity sensor

In order to measure the radius of curvature r , it is necessary to measure either the angular velocity ω or its square, ω^2 , simultaneously with the cable force F . By placing two single-axis accelerometers in line separated by a distance with their detector axes in

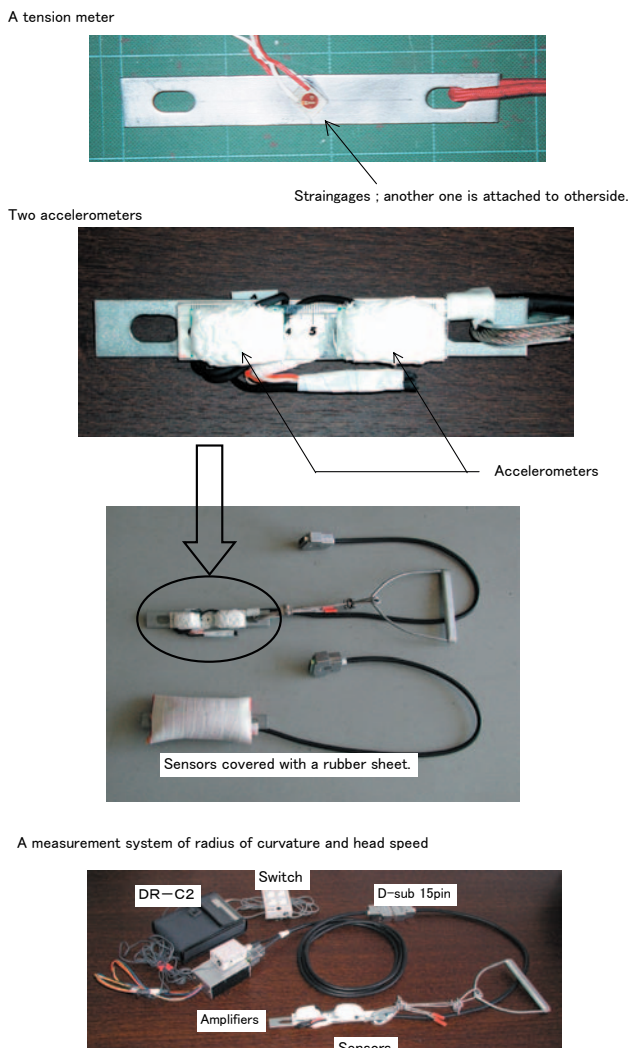


Figure 2 A sensor hammer consisting of a tension meter and accelerometers connected to amplifiers and a recorder.

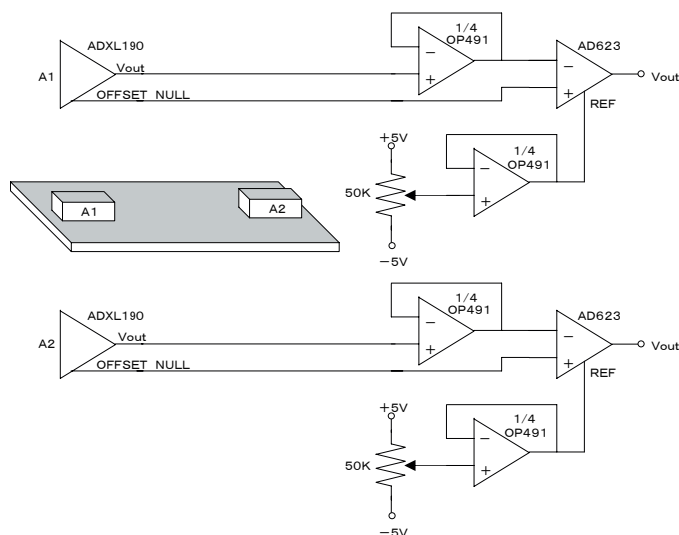


Figure 3 The electric circuit which consists in the amplifier of two accelerometers.

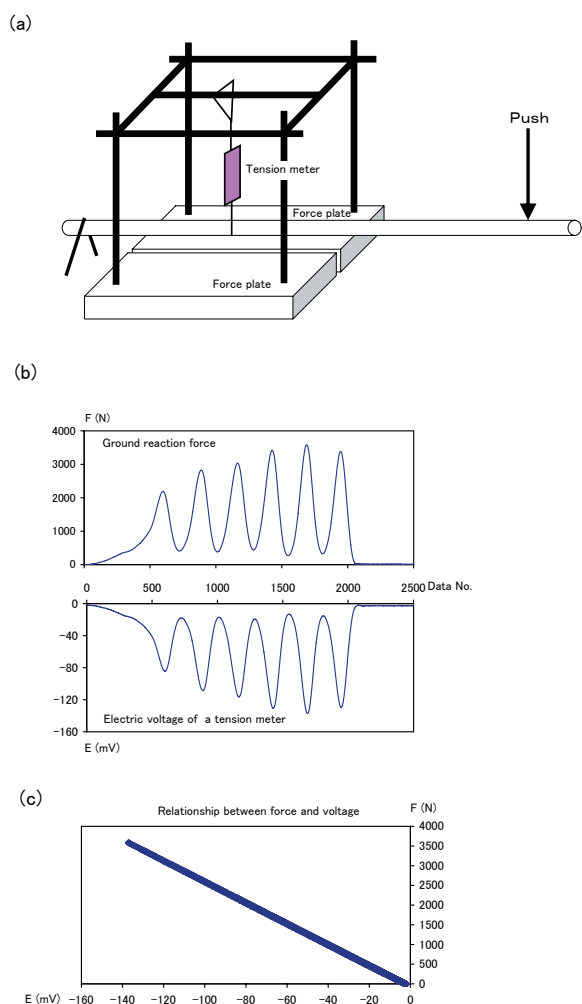


Figure 4 (a) is a sketch of calibration of a tension meter using force plates. Ground reaction forces and electric voltages of a sensor during calibration are shown in (b). (c) is the relationship between ground reaction forces and electric voltages.

agreement, we can measure the square of the angular velocity ω^2 by dividing the difference in acceleration between them $(a_1 - a_2)$ (m/s^2) by the distance between the accelerometers d (m) (Ohta, 1990).

$$\omega^2 = (a_1 - a_2) / d \quad (4)$$

By taking the difference between the two accelerometers, the acceleration components other than the centripetal force (translational acceleration and gravitational acceleration) cancel out. We used this method in the present research to measure the square of the angular velocity ω^2 .

We employed two small, lightweight single-axis accelerometers (ADXL 190: Analog Devices Corp.) for the angular velocity sensor used in the radius of curvature metering sensor developed for this research. We glued the accelerometers to an acrylic board 7 cm apart, and then attached them to a tension meter (Figure 2, center). We passed the signals from the 2 accelerometers through a circuit of our own design, as seen in Figure 3, and recorded them on the previously noted data recorder (Figure 2, bottom).

The combined weight of the hammer, radius of curvature sensor (tension sensor and angular velocity sensor), cord and cushioning material was 7.63 kg. Further, we considered the entire weight to belong to the hammer head rather than the handle, so we took the mass of the hammer m for Formulae (1), (2) and (3) to be 7.63kg.

2.2. Sensor adjustment method

2.2.1. Tension sensor

In the actual hammer throw, it has been reported that the hammer cable is subjected to a tensile force of 2750 N in a throw of 67.50 m (Dapena 1982), and a force of 3089 N in a throw of 79.47 m average (Okamoto et al. 1993). Therefore, as in Figure 4, we created equipment that adds strength to both the tension sensor and 2 force plates (Type 9281B: Kistler Corp.); using the lever principle, someone pushes a bar downwards, so that it can draw the homemade tension meter with a force greater than he can exert. By using this method, it is possible to adjust the tension to handle the 3000-4000 N that is in actuality likely to be exerted on the cable. The waveforms and correlation graphs of the tension sensor and force plates used in this research are shown in Figure 4. The slope of the regression line was -26.6054 (N/mV), and the coefficient of

correlation was -0.999 .

2.2.2. Acceleration sensor

The sensitivity of the accelerometers we used as angular velocity sensor is 19.0 (mv/G), according to the data supplied by the manufacturer (Analog Devices Corp.). In actuality, the sensitivity of each individual accelerometer varies from the nominal value, so a regression line was obtained by taking acceleration values of $+1G$, $0G$ and $-1G$ when making the detection axis of the accelerometer vertical downwards, horizontal, vertical upwards.

2.3. Experimental methodology

Subject was the present Japanese record holder ($83m47$ at time of experiment), with a four-rotation throw, height 187 cm, weight 97 kg, age 28 years. With an arm length of about 60 cm, length from the hammer head to the body when the hammer was maintained horizontal with a two-hand grip was approximately 180 cm.

Following sufficient warming up on the part of the subject, three throws were made indoors into a net 7.5 m from a circle. A shielded cable from the sensor was passed through a connector attached to the wrist of the left forearm (D-sub 15-pin, so that it would unplug with virtually no resistance upon release) and taped on the forearm, upper arm, shoulder and back; the data recorder was attached with a belt to the small of the back. The sampling frequency of the data recorder was 500 Hz.

Thrower and hammer movement were filmed with high speed video cameras (HSV-500C3: NAC Image Technology Corp.) stationed in three locations. Camera locations were facing the throw direction ($6m$ from center of circle) and left and right sides of the throw direction ($9-10m$ from center of circle). All 3 cameras were placed on tripods at circle level. All the cameras were synchronized; camera speed was 250 fps, and shutter speed was $1/1000$ s.

2.4. Analytical method

The tension F and square of the angular velocity ω^2 data recorded by the data recorder were attenuated to $125Hz$, and the data that were reversed in time and also reversed plus-minus were added to the original data and smoothed by using a fourth-order

Butterworth filter (Yamazaki and Yamamoto 1989). The square of the angular velocity data, in particular, were very noisy, so that it was necessary a low pass filter that could cut off sharply the components above the cut off frequency. We made the cut off frequency 6.25 Hz. Thus we obtained the radius of curvature r and speed v from the sensors using Formula (2) and Formula (3).

In addition, we were able to obtain the changes in position by using 3D image analysis (DLT method) by digitizing every other frame of the hammer head from the images taken by the 3 high-speed video cameras. The hammer head velocity could be obtained by taking the numerical differential of the various positional components (filtered by 11 point weighted moving average: cut off frequency approx. 11 Hz). Using the 11 point weighted moving average, it is not possible to obtain smoothed values for the 5 points at both ends, so for each of those 5 points the data used were the raw measurements. The velocity around the release can also be obtained. The radius of curvature R , original definition, was obtained by a pre-existing method from the altered-direction angle $\Delta \theta$ of the hammer head velocity and the movement distance Δs , as in Formula (5) (Yuasa et al. 1984).

$$R = \Delta s / \Delta \theta \quad (5)$$

The speed of the hammer head V is the magnitude of the velocity. In addition, the angular velocity Ω (rad/s) can be obtained using Formula (6).

$$\Omega = V / R \quad (6)$$

Using the high-speed video images, we measured the duration of operation from the beginning of rotation. We took the beginning of rotation to be the moment the turn began after two swings, and the end of operation to be the time that the hammer was released from the hand. For synchronization of sensor data and image data, we considered that it was synchronized at the moment when tension reached the zero point and could not be observed or became disconnected and the point on the video at which the connector appeared to be released, taking that moment to be 5.00 s.

3. Results

Of the three throws of the subject, we chose for research the one that image analysis of the speed of release revealed to be the greatest. Further, ignoring the effect of air resistance, we estimated that the

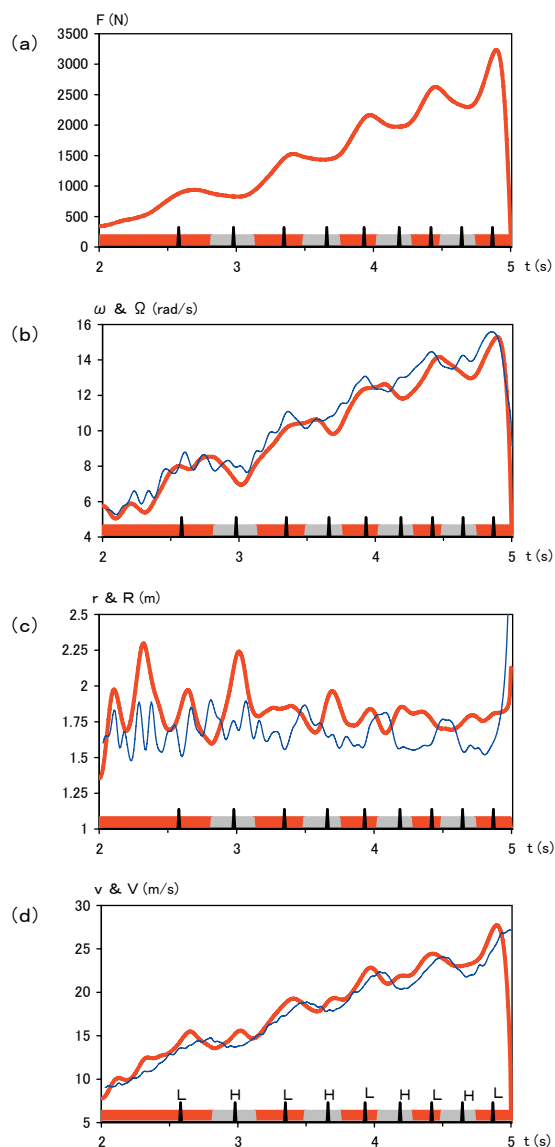


Figure 5 Graphs of cable force(a), angular velocity(b), radius of curvature(c) and speed of hammer head(d) with bars which indicate double support phases, single support phases, and instants of low or high points. The thick and red lines indicate ω , r and v measured by using the sensor hammer. The thin and blue lines indicate Ω , R and V measured by 3D analysis using video images. L is an instance about low point of hammer head, and H is an instance about high point. Red painted ranges are duration of double support phases, and gray painted ranges are duration of single support phases.

length of this throw would have been 75.33 m (initial speed 27.16 m/s, angle of release 38.26° , height of release 1.734 m).

Figure 5 shows (a) cable force, (b) angular velocity, (c) radius of curvature, (d) speed of hammer head, as obtained by the above-mentioned measurements and calculations. The thick and red lines on the graphs are sensor-obtained tension F ,

the angular velocity ω , the radius of curvature r , and the speed of hammer head v , while the thin and blue lines are the angular velocity Ω , the radius of curvature R and the speed of hammer head V as obtained from video analysis. The bottom of each graph shows the different intervals of the operational configuration observable during the hammer throw. The operational configurations delineated here are the phases supported by both legs (double support phases; red painted range), supported by one leg (single support phases; gray painted range) and the hammer head low point L and the high point H. The low point can be seen to occur in double support phases and the high point in single support phases.

Figure 6 shows average values of (a) cable force, (b) angular velocity, (c) radius of curvature, and (d) speed of hammer head. The red shaded marks are sensor-obtained tension F , angular velocity ω , radius of curvature r , speed of hammer head v , while the blue blank marks are angular velocity Ω , radius of curvature R , speed of hammer head V as obtained from video analysis. The average values are obtained for the duration that double support phase before low point (n:D.S.B.L.), double support phase after low point (n:D.S.A.L.), single support phase before high point (n:S.S.B.H.), single support phase after high point (n:S.S.A.H.) in each turn. Further, the n preceding each position is the number of turns. Based on these graphs, we outline below the most important results of the 4 measured items.

3.1. Tension

According to **Figure 5 (a)**, the tension F increases with the number of turns. In each turn, the tension increased in concert with the beginning of double support phase, with the tension reaching a peak from the low point up until the change to single support phase; a tendency for the tension to decrease in the following single support phase was observed. It can be seen from **Figure 6 (a)** that the average value was highest in each turn after the low point in double support phase (n:D.S.A.L.).

3.2. Angular velocity

As can be seen in **Figure 5 (b)**, the sensor-measured angular velocity ω increased in double support phases and decreased in single support phases, similarly to the tension. The activity

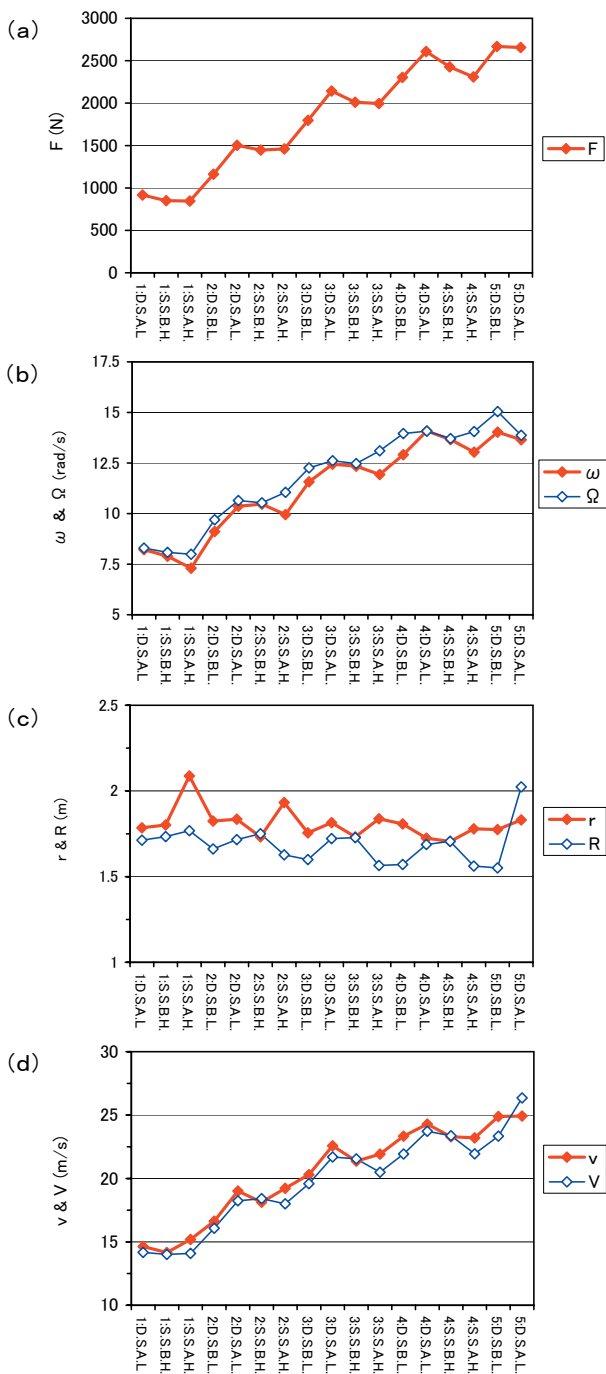


Figure 6 Graphs of cable force(a), angular velocity(b), radius of curvature(c) and hammer head velocity(d) measured by using sensor hammer (showed by red shaded marks), and measured by 3D analysis using video images (showed by blue blank marks). The marks show mean values which obtained for the duration that double support phases before low point (n:D.S.B.L.), double support phases after low point (n:D.S.A.L.), single support phases before high point (n:S.S.B.H.), single support phases after high point (n:S.S.A.H) in each turn. Further, the n preceding each position is the number of turn.

can be understood from **Figure 6 (b)**. The angular velocity obtained from the video images Ω showed changes in the angular velocity similar to the sensor's, but in turns 3 and 4, the angular velocity obtained from the video images reached a peak earlier. The above can be seen in **Figure 6 (b)**, from the fact that the video-obtained angular velocity Ω from turns 2 to 4 decreased slightly from double support phase after low point (n:D.S.A.L.) to single support phase before high point (n:S.S.B.H.), and increased in single support phase after high point (n:S.S.A.H.).

3.3. Radius of Curvature

According to **Figure 5 (c)**, the overall picture reveals that the radius of curvature obtained from the sensors r decreased in double support phases and increased in single support phases. The radius of curvature obtained from the video images R differed from r , increasing in double support phases and decreasing in single support phases. This can be seen in **Figure 6 (c)** as well. The radius of curvature obtained from the sensors was longer overall than that obtained from the video.

Further, in the latter part of the delivery phase (final double support phase), in the period between 0.05 to 0.1 s, the radius of curvature obtained from the video image suddenly grew longer.

3.4. Hammer head speed

According to **Figure 5(d)**, overall, the hammer head speed v obtained from the sensors gradually increased from the start of the turns to the low point of the delivery phase. Increases in speed were observed during double support phases, reaching peaks after the low points of double support phases. Thereafter, speed decreased slightly, with a tendency to increase from single support phases. Also in **Figure 6 (d)**, velocity decreased in each turn before the high point of single support phase (n:S.S.B.H.) and increased following the high point.

Comparing the speed V obtained from the video image with the speed v obtained from the sensors, according to **Figure 5 (d)**, a tendency was observed for the video image peak to be reached at a somewhat later point. Further, from **Figure 6 (d)** as well, it appeared that the video-obtained speed decreased overall in single support phase of each turn.

In addition, in the 0.1 s before release, the head

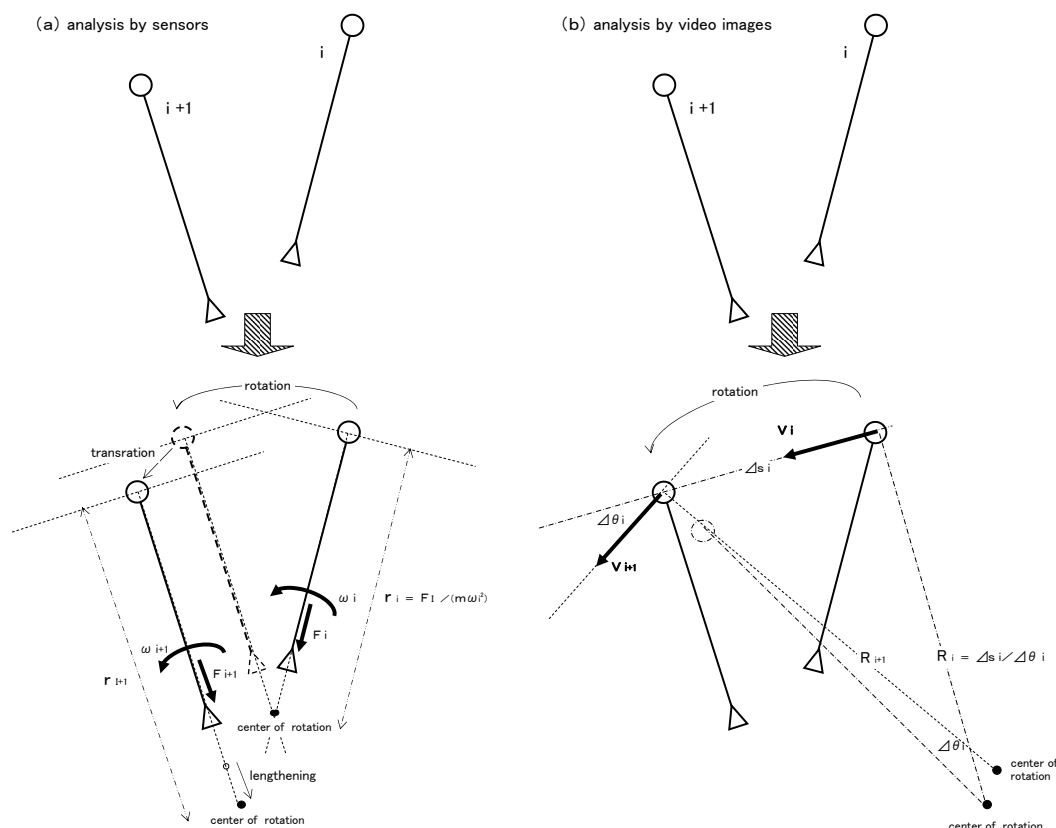


Figure 7 An explanation for sequential differences between a calculation of a radius of curvature measured by using the sensor hammer and a calculation measured by 3D analysis using video images.

speed obtained from the sensors differed from the actual speed obtained from the video, and a sudden decrease was observed.

4. Considerations

4.1. Characteristics of radius of curvature according to sensors

Kobayashi and Kaneko (1980) and Yuasa et al. (1984) calculated radius of curvature by 2D video analysis perpendicularly from above. Yuasa et al. in particular calculated from an analysis of a 73.37 m test throw by the then Japanese record holder. In these data, the radius of curvature varied greatly within the course of a single turn, from 1 m to 2.5 m. However, the radius of curvature obtained in this test from the sensors and the video images did not show such great changes as were observed in previous studies. It can be presumed that the radius of curvature measured from 3D imaging is more accurate than that of 2D imaging, so we believe that radius of curvature does not show radical changes,

but instead displays continual change.

Gutierrez et al. (2002) used originally defined methods to calculate radius of curvature by 3D video analysis for the top six male competitors and the top six female competitors (excluding no. 5) in the hammer throw at the Seville Athletics World Championship 1999, to obtain average values for single and double support phases for each turn. In all competitors, the length of the radius of curvature lengthened dramatically in the delivery phase, demonstrating results similar to our own video image radius of curvature. They reported as the reason for this that the throwers were moving in the same direction as the hammer as they moved from the low point to the release. In addition, in regard to the expansion and contraction of the radius, they noted differences among competitors, such as a tendency in some to increase the radius in single support phases and in others for the radius to decrease continuously with each turn, etc. The average value of the radius of curvature for each turn was in the range of 1.63-1.73 m, which was in close agreement with the 1.56-1.75 values obtained from video images in the

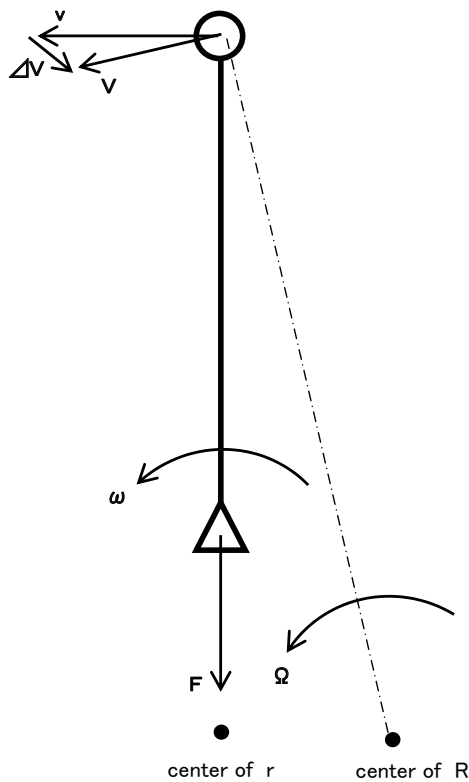


Figure 8 An explanation for a resultant difference between v which is an estimated velocity vector of hammer head measured by using the sensor hammer and V which is a velocity vector measured by 3D analysis using video images on a plane at an instance. ΔV indicates that a center of rotation (radius of curvature: r) has a translational element.

present study. However, these values obtained from video tend to be a bit smaller than the range obtained using the sensors (1.71-1.93 m). Further, the radius of curvature values obtained in this study exclude the values for the first turn.

In the measurement of angular velocity by two accelerometers, all acceleration but the centrifugal acceleration component is canceled by removing the differences in the two accelerations (Ohta et al. 1990). That is, the measurement of acceleration by the sensors can be considered to be the extraction of the rotational movement of the actual hammer only, as shown in **Figure 7 (a)**. On the other hand, in the video measurement, what is obtained is generally the movement path of the hammer head, so it includes both the rotational movement and the translational movement of the hammer. So the radius of curvature obtained to date from imaging has been a radius in which it was assumed that the path of the hammer head caused rotational movement only, as seen in

Figure 7 (b), but it has actually not taken only the actual rotational movement. What we are trying to say is that the radius of curvature measured by the sensors demonstrates the radius in the rotational movement more accurately than the video method.

4.2. Characteristics of hammer head speed according to sensors

Hammer head speed obtained by both sensor and video methods displayed a tendency to increase gradually while increasing and decreasing. The increasing tendency was particularly marked during double support phases. This corroborates with the experiential perceptions of competitors and coaches, who try to increase hammer speed during double support phases. On the other hand, the measurement using the metering sensor hammer we made for this research does not have the capability to obtain the speed at the time of release. Also, as seen in **Figure 8**, in comparing the hammer head speed obtained from the sensors with the actual speed obtained from the video images, not only the magnitude of the vector but the direction differed as well. The orientation of the hammer head speed v from the sensors was straight along the wire, but speed V from the video image was not always along the direction of the wire. We believe that the vector of differential between v and V ($\Delta V = V - v$) displays the translational speed of the radial center (the point at a distance of the radius of curvature r from the hammer head toward the wire), including the expansion and contraction rate of r .

Dapena and Feltner (1989) in trying to extract the rotational movement only from video analysis, introduced a quasi-inertial, non-rotating reference frame: R1 as the initial point of the thrower-hammer system center of gravity. In such cases as this, in order to obtain the center of gravity and the thrower-hammer system center of gravity, it becomes necessary to digitize multiple points on the body of the hammer thrower. Thus by analyzing the speed ($S_{H/R1}$) of the hammer head velocity ($V_{H/R1}$) relative to R1 and the speed ($S_{HC/R1}$) resulting from the cumulative effect of the cable force (F_{CT}) on the hammer head velocity relative to R1, $S_{H/R1}$ and $S_{HC/R1}$ begin to arise before the actual head speed from the latter half of single support phase, and are larger than the actual head speed until the first half of double support phase, growing smaller than the

actual head speed from the latter half of double support phase. Considering the translational movement of the thrower-hammer system to be the factor causing the increases and decreases in speed during turns, they obtained the speed as described above. In comparing the hammer head speeds obtained by the sensors and those obtained by the video in this research, we see that V obtained from the video is larger in the first half of single support phase, while in other phases the sensor value v is larger. If we think of the sensor value as $S_{H/R1}$, and that from the video as the actual head speed, we can infer by analogy with the previous researches that the sensor measurement represents the rotational movement component of the thrower-hammer system.

However, because the model used in this research deals only with hammer movement, differing from the hammer-throw model used in their research, the center of pass assumed from the radius of curvature is neither strictly the thrower-hammer system center of gravity nor the individual center of gravity. However, by measuring only angular velocity of the rotational movement of the hammer, sensor measurement permits obtaining the speed with the translational movement of the hammer in the sensor measurement model factored out, which we think will shorten data processing time.

4.3. Future issues

By using the sensor hammer, it has become possible to make direct measurements of cable tension and angular velocity, enabling rapid data processing and analysis quickly after data collection. Further, by improving data processing procedures and methods of displaying results, we hope to achieve construction of a system that will permit reduction of the results at the athlete-coach level. Coaching to date has consisted of reliance on language, looking at video or stills after practice and judging the quality of the movements. However, if operational and mechanical conditions could be shown, for example by sound volume or sound type or frequency, and information could be had on the spot at the time of performing the sport, we believe that it would become possible to gain better techniques faster.

However, the sensor-measured radius of curvature differs from the original definition of radius of curvature. Further, the measurements let us find only the rotational movement of the hammer using

accelerometers, but in tension, not only the rotational but the translational movement is included. Also, the center of pass inferred from the radius of curvature is not strictly the body center of gravity nor the thrower-hammer system center of gravity. In this regard, even if we are able to understand the actual movement of the hammer from the sensor data, it does not mean that we understand the movement of the thrower. However, since we think it permits us sufficient understanding of the characteristics of hammer movement, we should collect profiling data for many test subjects.

5. Summary

In this research, we built a sensor hammer to measure cable tension and the square of the angular velocity at throw time. We conducted a basic research, calculating tension, angular velocity, radius of curvature and hammer head speed from this sensor in order to establish a method that permits real-time feedback. The test subject of this research was the Japanese record holder in the hammer throw.

Tension, angular velocity and speed increased gradually with each turn, but there was a tendency for increases to occur during double support phases. Radius of curvature increased during single support phases and showed a tendency to decrease during double support phases. Measurement of angular velocity by the sensor takes only the rotational movement of the hammer movement, so that although the radius of curvature obtained, when compared to previous results, differs slightly not only in length of radius but also in the position of the center of pass, we believe that reasonable results were obtained. On the other hand, in regard to speed of the hammer head, even though we could not obtain its magnitude at release, we were able to obtain approximate changes during the throwing operation in a short time.

References

- Dapena, J. (1982). Tangential and perpendicular forces in the hammer throw. *Hammer Notes*, 5 : 40-42.
- Dapena, J. (1984). The pattern of hammer speed during a hammer throw and influence of gravity on its fluctuations. *Journal of biomechanics*, 17 : 553-559.
- Dapena, J. (1985). Factors affecting the fluctuations of hammer speed in a throw. In Winter, D.A. et al. (eds.), *Biomechanics I X -B*. (pp. 499-503). Human Kinetics, Champaign, IL.

- Dapena, J. and Feltner, M.E. (1989). Influence of the direction of the cable force and of the radius of the hammer path on speed fluctuations during hammer throwing. *Journal of biomechanics*, 22 : 565-575.
- Dyson, G. (1972). *The mechanics of athletics* (fifth ed.). In Kinpara, I. et al. (trans.). (pp. 231-237). Tokyo: Taishukan Publishing Co., Ltd. (In Japanese).
- Gutierrez, M., Soto, V.M. and Rojas, F.J. (2002). A biomechanical analysis of the individual techniques of the hammer throw finalists in the Seville Athletics World Championship 1999. *New Studies in Athletics*, 17 : 15-26.
- Ikegami, Y., Sakurai, S., Okamoto, A., Ueya, K. and Nakamura, K. (1994). Biomechanical analysis of hammer throw. In Sasaki, H. et al. (eds.), *How they ran, jumped and threw. The report on the 3rd Athletics World Championship 1991 in Tokyo* (pp. 240-256). Tokyo: Baseball Magazine Sha Co., Ltd. (In Japanese).
- Kobayashi, K. and Kaneko, K. (1980). Mechanics of hammer throw. *Journal of Health, Physical Education and Recreation*, 30 : 499-503. (In Japanese).
- Lapp, V.W. (1935). A study of hammer velocity and physical factors involved in hammer throwing. *The research quarterly of the American Physical Education Association*. VI (3) Supplement : 134-144.
- Murofushi, S., Saito, M. and Yuasa, K. (1982). Biomechanical analysis of hammer throw: The speed, height and angle of release and phasic analysis. *Research journal of physical education Chukyo University*, 23 : 38-43. (In Japanese).
- Murofushi, S. (1994). *Hammer throw*. (pp. 30-52). Tokyo: Baseball Magazine Sha Co., Ltd. (In Japanese).
- Ohta, K., Kobayashi, K. and Doi, Y. (1990). A process of analysis of acceleration on accelerative coordinate system: Mechanical analysis of smashing movement in badminton. In Japanese Society of Biomechanics (ed.), *BIOMECHANICS 1990* (pp. 135-139). Tokyo: Medical Press Inc. (In Japanese).
- Okamoto, A., Sakurai, S. and Ikegami, Y. (1993). Mechanical analysis of hammer throw: 2nd report of 3D analysis in 3rd Athletics World Championship. *The proceedings of the 44th annual convention in Japanese Society of Physical Education A* (pp. 405). (In Japanese).
- Ono, K. (1957). *The mechanics of athletics*. (pp.168-174). Tokyo: Dobun-shoin. (In Japanese).
- Payne, H. (1990). *The mechanics of hammer throwing. Techniques in Athletics*. Cologne 7-9 June 1990 : 149-197.
- Umegaki, K. and Mizutani, Y. (1997). Acceleration of the hammer-head relative to the thrower. *Research journal of physical education Chukyo University*, 38 : 53-63. (In Japanese).
- Yamazaki, N. and Yamamoto, S. (1989). Smoothing. In Tsuchiya, K. (ed.), *A text book on clinical analysis of walking* (pp. 32-35). Tokyo: Ishiyaku Publishers, Inc. (In Japanese).
- Yuasa, K., Okuyama, H., Murofushi, S. and Saito, M. (1984). Biomechanical characteristics of hammer throwing. *Journal of Health, Physical Education and Recreation*, 34 : 319-322. (In Japanese).



Name:
Koji MUROFUSHI

Affiliation:
Chukyo University Graduate School of Health and Sport Sciences

Address:

101 Tokodachi, Kaizu-cho, Toyota, Aichi 470-0393 Japan

Brief Biographical History:

1997-Master's Degree Program in Graduate School of Health and Sport Sciences, Chukyo University.

1999-Doctorate Degree Program in Graduate School of Health and Sport Sciences, Chukyo University. (Ph.D.candidate)

Main Works:

- “The electronic measurement of the radius of curvature in the case of the hammer throw.” Master’s thesis of Chukyo University(1999). (In Japanese).

Membership in Learned Societies:

- Japan Society of Physical Education, Health and Sport Sciences.
- Japanese Society of Biomechanics.

Appendix

For ease of understanding, we conveniently offer explanation of a two-dimensional plane, but it does not differ substantially from three-dimensions. As shown in **Figure A**, **V** is the velocity vector of the particle P, **F** is the force vector exerted on the particle P. In addition, **r** is the position vector of P. **t** is the unit vector of the tangential direction, and it faces in the same direction as **V**. **n** is the unit vector of the normal direction. **F** and **V** are shown below as constituents of the unit vectors.

$$\begin{aligned} \mathbf{F} &= F_t \mathbf{t} + F_n \mathbf{n} \\ \mathbf{V} &= V \mathbf{t} \end{aligned} \tag{A-1}$$

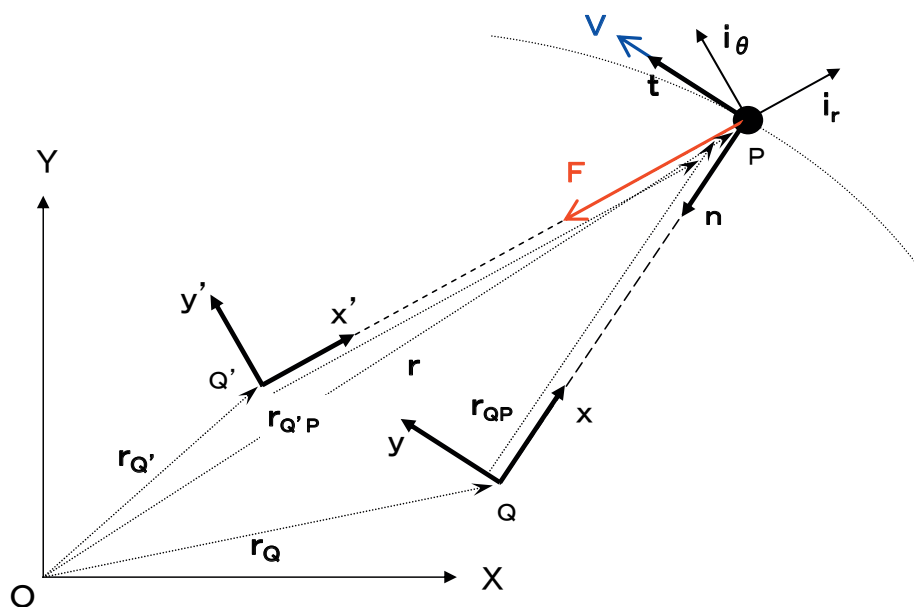


Figure A Diagram indicate movement of a particle P (mass : m) shown by tangential (unit vector : **t**) and normal(unit vector : **n**) components, or shown by radial (unit vector : **i_r**) and rotational (unit vector : **i_θ**) components. **F** is a force vector and **V** is a velocity vector of P. A point Q is a center of rotation of R which means normal components from P, and Q' is a center of rotation of r which means radial component from P at an instance. **r** is a displacement vector of P.

Radius of curvature R, according to the original definition, can be obtained by the following formula, on the assumption that circular movement arises in this instant. m is the mass of P.

$$F_n = (m V^2) / R \tag{A-2}$$

The point Q at a distance R from the particle P in the normal direction (**n** direction) is the center of pass. If the route of the particle P is smooth, the length of radius of curvature R and center of pass position Q will change, but the change can be considered to be continuous. We take Q as the starting point for the y-axis in the tangential direction (**t** direction) and backward normal direction (**- n** direction) for the x-axis. If we take the rotational movement of the movement coordinate system Qxy as Ω , then the velocity of particle P seen from Q is

$$d\mathbf{r}_{QP}/dt = - dR/dt \mathbf{n} + R \Omega \mathbf{t} \tag{A-3}$$

From the definition of radius of curvature, we get

$$\begin{aligned} V &= R \Omega \\ \mathbf{V} &= d\mathbf{r}/dt = R \Omega \mathbf{t} \end{aligned} \tag{A-4}$$

Concomitantly, the velocity of Q seen from the fixed coordinate system OXY is

$$d\mathbf{r}_Q/dt = d\mathbf{r}/dt - d\mathbf{r}_{QP}/dt = \mathbf{V} - d\mathbf{r}_{QP}/dt$$

If we substitute (A-3) and (A-4) in the right hand side of the above formula, we get

$$d\mathbf{r}_Q/dt = dR/dt \mathbf{n} \tag{A-5}$$

Concomitantly, Q contains the translational component of the magnitude of the contraction and expansion rate of the radius in the normal direction.

We take the unit vector facing in the opposite direction from **F** as **i_r**, and the unit vector that crosses it as **i_θ**. **F** is shown as follows using the unit vector component.

$$\mathbf{F} = F \mathbf{i}_r$$

If we take the rate of change in the direction of \mathbf{F} as ω and the radius assumed at the instant circular movement begins as the radius of curvature r in this research, we can obtain F as in the formula below.

$$F = m r \omega^2 \quad (\text{A-6})$$

The significance of obtaining the radius of curvature using F and ω is that it let us grasp the characteristics of hammer movement using what can be measured by the sensor.

The point Q' at a distance r in the F direction ($-\mathbf{i}_r$ direction) is the center of pass defined in this research. Taking Q' as the starting point, the \mathbf{i}_r direction is the x' axis and the \mathbf{i}_θ is the y' axis. The velocity of P seen from Q' is

$$d\mathbf{r}_{Q'P}/dt = dr/dt \mathbf{i}_r + r \omega \mathbf{i}_\theta \quad (\text{A-7})$$

Concomitantly, the velocity of Q' seen from the fixed coordinate system OXY is

$$d\mathbf{r}_{Q'}/dt = d\mathbf{r}/dt - d\mathbf{r}_{Q'P}/dt = \mathbf{V} - d\mathbf{r}_{Q'P}/dt$$

Substituting (A-1) and (A-7) in the right-hand side of the formula, we get

$$d\mathbf{r}_{Q'}/dt = \mathbf{V} \mathbf{t} - dr/dt \mathbf{i}_r - r \omega \mathbf{i}_\theta \quad (\text{A-8})$$

Concomitantly, Q' contains the expansion and contraction rate of the radius of curvature ($-dr/dt \mathbf{i}_r$) and the translational component of the differential in velocity assumed by the actual velocity and the estimated velocity by sensor ($\mathbf{V} \mathbf{t} - r \omega \mathbf{i}_\theta$).

As seen above, the definition by the sensor used in this research and previous definitions differ in Formulas (A-2) and (A-6) concerning the way of obtaining radius of curvature, but differ concerning center of pass movement in Formulas (A-5) and (A-8).